

# cs171: Final Project

Patrick O'Brien, Katy Wyman, Daniel Schultz

<http://chandra.phptime.biz/>

# cs171: Final Project

Process Book  
2014

# cs171: Final Project



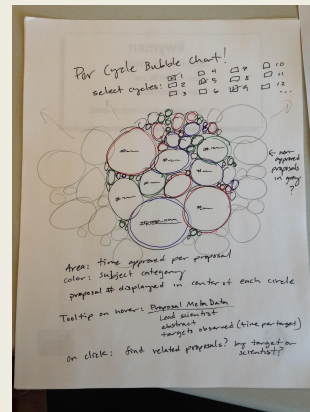
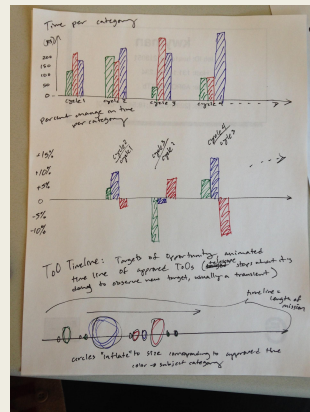
## Chandra -- Eye to the Sky

Eye to the Sky visualizes the research and exploration enabled by the Chandra Space Telescope.

# Initial Project Proposal

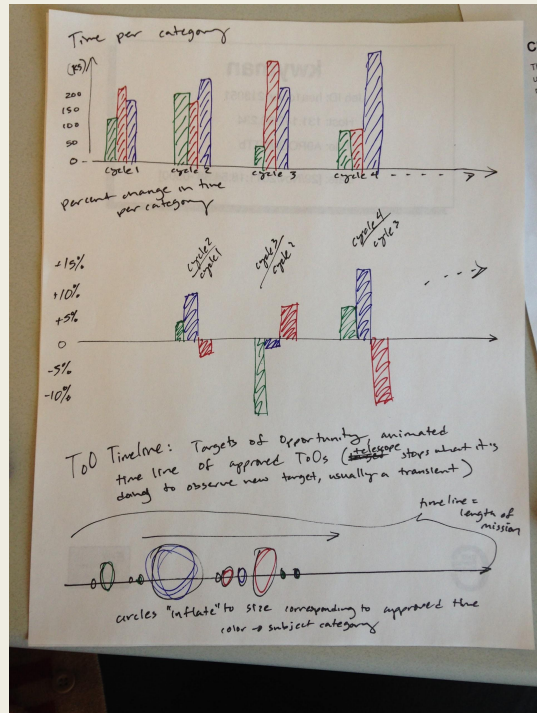
## Summary

We aim to create a visual representation of science categories and the time-resource allocation of the telescope, along with providing an engaging visual experience to share the joy of the cosmos with others who might find such data inaccessible.



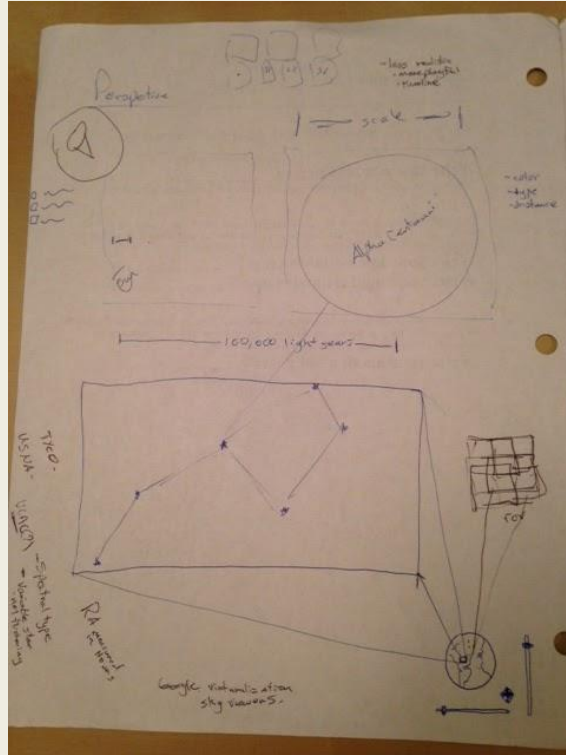
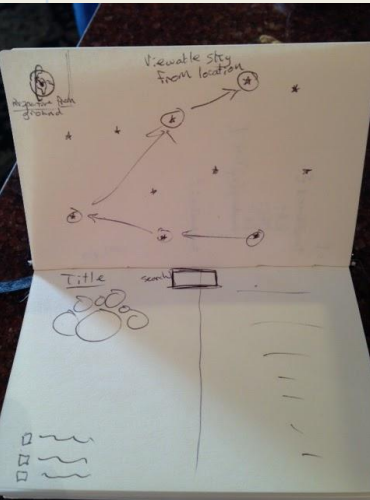
Initial concept sketches of visualization

# Project Evolution



Initial sketches focused on the raw data behind Chandra resource allocation paired with rudimentary bar graphs and data representations (pictured on the top), including a timeline of special type of Chandra observations (pictured at bottom).

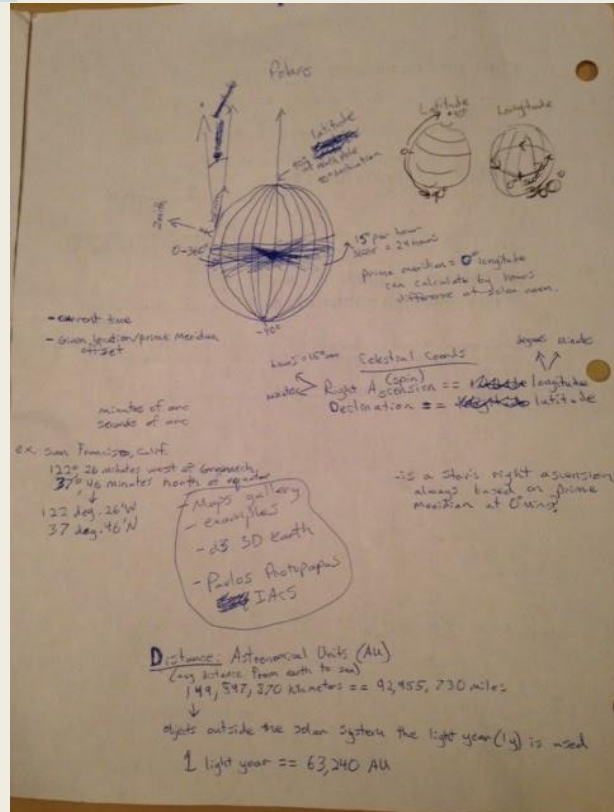
# Project Evolution



Evolutions of the concept focused on using a D3 generated globe and a rectangular field of view on which stars and their data could be represented. This presented problems translating 3D spatial coordinates accurately onto a 2D rectangle.

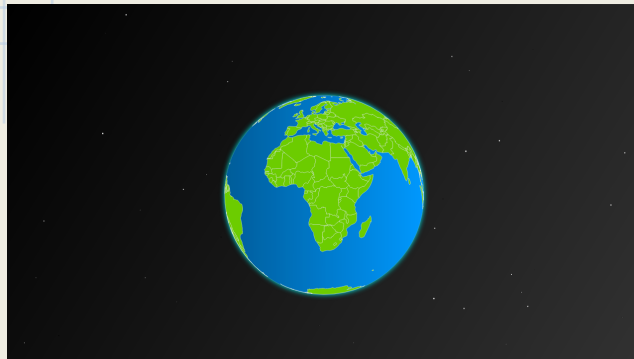
Pat met with Pavlos Protopapas, IACS Scientific Program Director Lecturer to discuss the feasibility of our visualization. Talking with Pavlos helped us discover some of the difficulties and limitations in our approach. As a result we decided to plot and display points based upon a single Latitudinal, Longitudinal point rather than a window of four bounding points.

# Evolution

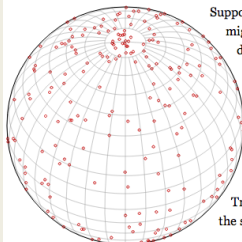


Pavlos also mentioned that star size and distance estimate information was only available for a handful of stars, making a key aspect of our initial plan, to compare the size of our sun to distant stars, difficult and impractical.

# Project Evolution



## Random Points on a Sphere



Suppose we want to generate uniformly distributed points on a sphere. You might start off by picking spherical coordinates  $(\lambda, \phi)$  from two uniform distributions,  $\lambda \in [-180^\circ, 180^\circ]$  and  $\phi \in [-90^\circ, 90^\circ]$ .

However, we can quickly see that this will result in an uneven distribution, with the density increasing as we get closer to the poles.

One way to explain this is to look at how the area of a given "square" of width  $\Delta\lambda$  and height  $\Delta\phi$  varies with  $\phi$ .

Try picking any square on the graticule (the spherical grid). See how the squares get smaller towards the poles?

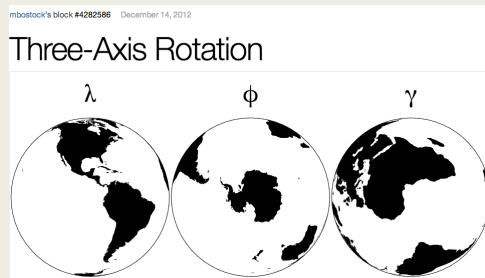
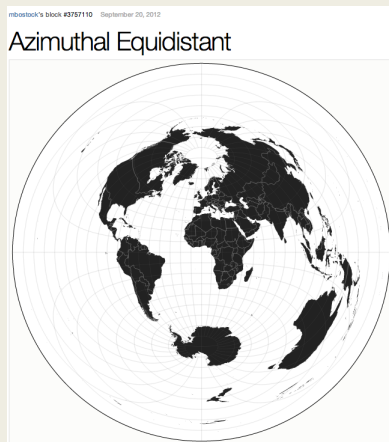
Inspired by a D3 generated globe with randomly generated stars, the bar charts and initial visual representation were replaced with a 3D representation of the earth, with stars drawn on the inside of a larger, invisible sphere. This prevents distortion, provides a more stimulating visual experience, and translates better to the underlying dataset provided by the Chandra program.

(<http://marcneuwirth.com/blog/2012/06/24/creating-the-earth-with-d3-js/>)

(<http://www.jasondavies.com/maps/random-points/>)



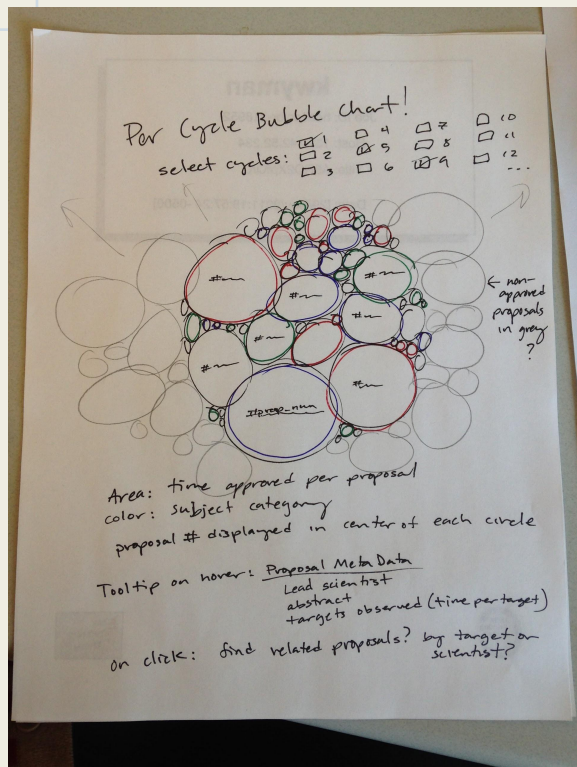
# Project Inspiration



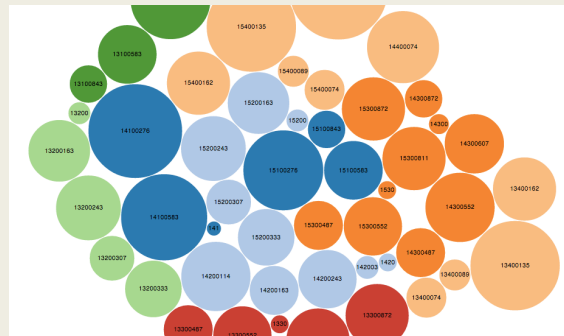
Fortunately, there were many examples by mbostock of global projections, along with examples of 3 axis of rotation, Azimuthal, and Orthographic representations of the earth.

(<https://github.com/mbostock/d3/wiki/Geo-Projections>)

# Communicating Data



While visually stimulating, the 3D globe and starscape limited our ability to represent the underlying data we had access to, and we drafted designs for a bubble chart to better represent resource allocation of the Chandra telescope while still allowing for the 3D visual.



# Data Collection

**Subject Category:** STARS AND WD

**Proposal Number:** 15200243

**Title:** Rejuvenation of the Innocent Bystander: Testing Spin-Up in Dwarf Carbon Stars

**Type:** GO **Total Time (ks):** 104.6

**PI Name:** Paul Green

Carbon stars (C-O) were long assumed to all be giants, because only AGB stars dredge up significant carbon into their atmospheres. We now know that dwarf carbon (dC) stars are actually far more common than C giants. These dCs are hypothesized to have accreted C-rich envelope material from an AGB companion, in systems that have likely undergone a planetary nebula phase, eventually yielding a white dwarf and a dC that has gained both significant mass and angular momentum. To test whether the X-ray emission strength and spectral properties are consistent with a rejuvenated dynamo, we propose a Chandra pilot study of dCs selected from the SDSS; some have hot white dwarf companions (indicating more recent mass transfer), and all show Balmer emission lines (a sign of activity).

R.A.	Dec.	Target Name	Det.	Grating	Exp.Time (ks)
10:15:48.90	+09:46:49.80	SDSS J101548.90+094649.7	ACIS-S	NONE	16.1

**Subject Category:** STARS AND WD

**Proposal Number:** 15200307

**Title:** Catching an FUor in the Act: Chandra ToO Observations of Extreme Accretion onto Young Stars

**Type:** TOO **Total Time (ks):** 50

**PI Name:** David Pooley

FU Orionis (FUor) outbursts are a transitory rapid accretion phase in the evolution of young stellar objects. We propose to obtain an X-ray spectrum during the rise to peak brightness of an FUor with Chandra. This phase has never been observed in X-rays and could reveal important information about the nature and source of the X-ray emission in these objects. In particular, it would provide a unique test of whether high-velocity jets are formed during the intense accretion event. These jets are expected to form X-ray dissociation regions, and X-ray emission does correlate with outflows from young stellar objects. If these jets only exist during the high levels of accretion during the rise to peak brightness, as they are thought to, X-ray observations during this time are crucial.

R.A.	Dec.	Target Name	Det.	Grating	Exp.Time (ks)
		FUor Outburst	ACIS-S	NONE	50

Initially, the data was going to be scraped from numerous web pages, consolidated, and processed into a CSV for use in D3.

The lack of proper underlying structure on the web pages combined with the decentralized form of the data proved to be difficult to scrape.

([http://cxc.harvard.edu/target\\_lists/cycle15/allproposals15.html](http://cxc.harvard.edu/target_lists/cycle15/allproposals15.html))

# Data Wrangling

```
ra      dec      approved_exposure_time  proposal_id  targname
title
abstract
      approved_time      last      first
ENDHEADERS
      166.113333 $%      38.208806 $%      30.000000 $%      14361 $% Mkn421
A0-13 Calibration Observation of Mkn421 to Monitor the Contaminant on the ACIS Filter
There is some evidence that the growth rate of the contaminant on the edges of the ACIS filters is changing. This observation
$%      60.000000 $% McCluskey, Jr.      $% George      14361 $% Mkn421
166.113333 $%      38.208806 $%      30.000000 $%      14361 $% Mkn421
A0-13 Calibration Observation of Mkn421 to Monitor the Contaminant on the ACIS Filter
There is some evidence that the growth rate of the contaminant on the edges of the ACIS filters is changing. This observation
$%      85.000000 $% McCluskey, Jr.      $% George      14361 $% Mkn421
166.113333 $%      38.208806 $%      30.000000 $%      14361 $% Mkn421
A0-13 Calibration Observation of Mkn421 to Monitor the Contaminant on the ACIS Filter
There is some evidence that the growth rate of the contaminant on the edges of the ACIS filters is changing. This observation
$%      40.000000 $% McCluskey, Jr.      $% George      14361 $% Mkn421
166.113333 $%      38.208806 $%      30.000000 $%      14361 $% Mkn421
A0-13 Calibration Observation of Mkn421 to Monitor the Contaminant on the ACIS Filter
There is some evidence that the growth rate of the contaminant on the edges of the ACIS filters is changing. This observation
$%      70.000000 $% McCluskey, Jr.      $% George      14361 $% Mkn421
166.113333 $%      38.208806 $%      30.000000 $%      14361 $% Mkn421
A0-13 Calibration Observation of Mkn421 to Monitor the Contaminant on the ACIS Filter
There is some evidence that the growth rate of the contaminant on the edges of the ACIS filters is changing. This observation
$%      37.000000 $% McCluskey, Jr.      $% George      14361 $% Mkn421
166.113333 $%      38.208806 $%      30.000000 $%      14361 $% Mkn421
A0-13 Calibration Observation of Mkn421 to Monitor the Contaminant on the ACIS Filter
There is some evidence that the growth rate of the contaminant on the edges of the ACIS filters is changing. This observation
$%      20.000000 $% McCluskey, Jr.      $% George      14361 $% Mkn421
166.113333 $%      38.208806 $%      30.000000 $%      14361 $% Mkn421
A0-13 Calibration Observation of Mkn421 to Monitor the Contaminant on the ACIS Filter
There is some evidence that the growth rate of the contaminant on the edges of the ACIS filters is changing. This observation
$%      50.000000 $% McCluskey, Jr.      $% George      14361 $% Mkn421
166.113333 $%      38.208806 $%      30.000000 $%      14361 $% Mkn421
A0-13 Calibration Observation of Mkn421 to Monitor the Contaminant on the ACIS Filter
There is some evidence that the growth rate of the contaminant on the edges of the ACIS filters is changing. This observation
```

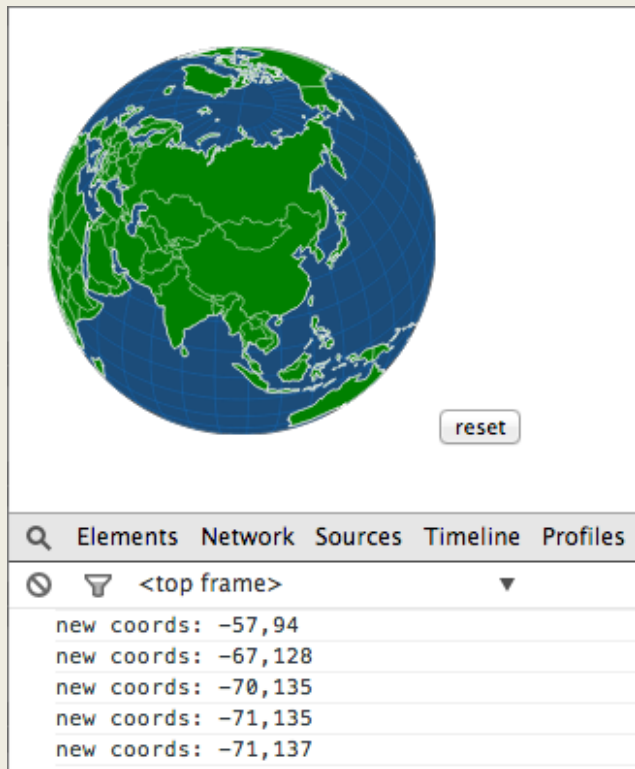
Instead, the data was taken directly from the database, which, unfortunately lacked elegant export functionality. The data was dumped into poorly formatted text files that had to be processed programmatically.

# Data Wrangling

```
4257 146.917500|-30.948889|50.000000|6569|MCG -5-23-16|ACTIVE GALAXIES AND QUASARS|GO|Revealing the Relativistic Iron Line in the S
4258 172.130000|58.561306|10.000000|6577|NGC 3690|ACTIVE GALAXIES AND QUASARS|DDT|An accretion eruption in the western nucleus of A
4259 75.217083|-70.771000|3.500000|7595|IGR J05007-7047|ACTIVE GALAXIES AND QUASARS|DDT|Search for strongly obscured AGNs: support
4260 119.070000|-41.635000|3.500000|7595|IGR J05763-4137|ACTIVE GALAXIES AND QUASARS|DDT|Search for strongly obscured AGNs: support
4261 156.267083|-68.483000|3.500000|7595|IGR J10252-6829|ACTIVE GALAXIES AND QUASARS|DDT|Search for strongly obscured AGNs: support
4262 167.144167|-51.014000|3.500000|7595|IGR J11085-5100|ACTIVE GALAXIES AND QUASARS|DDT|Search for strongly obscured AGNs: support
4263 180.657083|-53.816000|3.500000|7595|IGR J12026-5349|ACTIVE GALAXIES AND QUASARS|DDT|Search for strongly obscured AGNs: support
4264 197.267083|11.622000|3.500000|7595|IGR J13091+1137|ACTIVE GALAXIES AND QUASARS|DDT|Search for strongly obscured AGNs: support
4265 296.835833|44.864000|3.500000|7595|IGR J19473+4452|ACTIVE GALAXIES AND QUASARS|DDT|Search for strongly obscured AGNs: support
4266 189.780000|-16.196000|3.500000|7595|IGR J12391-1612|ACTIVE GALAXIES AND QUASARS|DDT|Search for strongly obscured AGNs: support
4267 37.610833|18.606111|70.000000|6414|c10230+1836|CLUSTERS OF GALAXIES|LP|DARK ENERGY WITH X-RAY CLUSTERS: CHANDRA OBSERVATIONS O
4268 52.150417|-21.667778|60.000000|6414|c10328-2140|CLUSTERS OF GALAXIES|LP|DARK ENERGY WITH X-RAY CLUSTERS: CHANDRA OBSERVATIONS
4269 61.351250|-41.004167|80.000000|6414|c10405-4100|CLUSTERS OF GALAXIES|LP|DARK ENERGY WITH X-RAY CLUSTERS: CHANDRA OBSERVATIONS
4270 80.293750|-25.510000|15.000000|6414|c10521-2530|CLUSTERS OF GALAXIES|LP|DARK ENERGY WITH X-RAY CLUSTERS: CHANDRA OBSERVATIONS
4271 149.011667|41.118889|40.000000|6414|c10956+4107|CLUSTERS OF GALAXIES|LP|DARK ENERGY WITH X-RAY CLUSTERS: CHANDRA OBSERVATIONS
4272 34.140417|-17.790833|65.000000|6414|c10216-1747|CLUSTERS OF GALAXIES|LP|DARK ENERGY WITH X-RAY CLUSTERS: CHANDRA OBSERVATIONS
4273 58.997083|-37.696111|30.000000|6414|c10355-3741|CLUSTERS OF GALAXIES|LP|DARK ENERGY WITH X-RAY CLUSTERS: CHANDRA OBSERVATIONS
4274 7.640000|26.304444|20.000000|6414|c10030+2618|CLUSTERS OF GALAXIES|LP|DARK ENERGY WITH X-RAY CLUSTERS: CHANDRA OBSERVATIONS OF
4275 209.330833|62.545000|45.000000|6414|c11357+6232|CLUSTERS OF GALAXIES|LP|DARK ENERGY WITH X-RAY CLUSTERS: CHANDRA OBSERVATIONS
4276 133.305833|57.995556|25.000000|6414|c10853+5759|CLUSTERS OF GALAXIES|LP|DARK ENERGY WITH X-RAY CLUSTERS: CHANDRA OBSERVATIONS
4277 185.507917|27.155278|50.000000|6414|c11222+2709|CLUSTERS OF GALAXIES|LP|DARK ENERGY WITH X-RAY CLUSTERS: CHANDRA OBSERVATIONS
4278 183.080000|27.553611|15.000000|6414|c11212+2733|CLUSTERS OF GALAXIES|LP|DARK ENERGY WITH X-RAY CLUSTERS: CHANDRA OBSERVATIONS
4279 180.557083|57.864722|60.000000|6414|c11202+5751|CLUSTERS OF GALAXIES|LP|DARK ENERGY WITH X-RAY CLUSTERS: CHANDRA OBSERVATIONS
4280 53.292917|-24.944444|40.000000|6414|c10333-2456|CLUSTERS OF GALAXIES|LP|DARK ENERGY WITH X-RAY CLUSTERS: CHANDRA OBSERVATIONS
4281 303.211667|-56.848306|450.000000|6413|Abell 3667|CLUSTERS OF GALAXIES|LP|A CHANDRA TREASURY OBSERVATION OF THE BEST EXAMPLE OF
4282 349.974583|0.636556|75.000000|6404|RC52319.9+0030|CLUSTERS OF GALAXIES|GO|Cluster Strong Lensing at High Redshift|06800198|The
4283 283.034583|57.195417|30.000000|6400|RXC J1052.1+5711|CLUSTERS OF GALAXIES|GO|Chandra observations of clusters of galaxies cont
4284 2.833333|-28.871944|20.000000|6458|2PIGG20.061 J0011.5-2850|CLUSTERS OF GALAXIES|GO|X-ray Properties of a Mass-Selected Group
4285 336.954167|-30.577778|22.000000|6458|2PIGG20.058 J2227.0-3041|CLUSTERS OF GALAXIES|GO|X-ray Properties of a Mass-Selected Group
4286 47.858333|-26.928889|40.000000|6458|2PIGG20.068 J0311.8-2655|CLUSTERS OF GALAXIES|GO|X-ray Properties of a Mass-Selected Group
```

The result was a D3-friendly delimited file of over 6000 entries which could be further processed by D3 to power our visualization.

# Implementation



Initial D3 implementation of the Earth, supporting mouse movement and calculating the latitude and longitude of the viewer's perspective. This calculation was necessary to ensure that the starscape would be accurately mapped based on the user's chosen location.

# Calculating the view

**Math behind some simple azimuthal projections:** Almost all projections (and all azimuthal ones) assume that you begin with a central point, (ra0, dec0), which happens to match the center of your chart. In an azimuthal projection, if you measure an azimuth (or, to use the celestial rather than the cartographic term, a position angle) from this point, you get a correct result. Distortions in the rest of the sky mean that this is the `_only_` point for which this holds true.

In addition to this central point, you've got a point (ra, dec) that you want to project, resulting in a "plane" point (x, y). Here goes:

```
delta_ra = ra - ra0;          /* determine difference in RA */
x1 = cos( dec ) * sin( delta_ra );
y1 = sin( dec ) * cos( dec0 ) - cos( dec ) * cos( delta_ra ) * sin( dec0 );
```

Two side points:

- (1) You could set `x = x1`, `y = y1`, do no more work, and have an orthographic projection.
- (2) For a given chart, you'll run through bazillions of (ra, dec) values, while (ra0, dec0) stays constant. So it can pay to save math by computing the sines and cosines of ra0 and dec0 "up front", before you plot a single star. (This used to be absurdly important in the Bad Old Days before math chips became common. It's not so important now, but it's still a good idea.)

```
z1 = sin( dec ) * sin( dec0 ) + cos( dec ) * cos( dec0 ) * cos( delta_ra );
```

Physically speaking, we're treating the celestial sphere as if it were a ball held at infinity, and we've put Cartesian axes in it. We're staring down at (ra0, dec0), and the Z axis points from the center of the ball, up through (ra0, dec0), and through us. So a point at `z1 = -1` would be on the exact far side of the ball, at (ra0 - 180 degrees, -dec0); a point at `z1 = 0` would be on the "horizon" (edge) of the ball, as seen by us; and a point at `z1 = 1` would be on the near side of the ball, as seen by us.

The result is that (x1, y1, z1) is a unit vector. (ra0, dec0) gets mapped to (0, 0, 1). (ra0 + 180, -dec0) gets mapped to (0, 0, -1). (ra0 + 90, 0) gets mapped to (1, 0, 0). And so on.

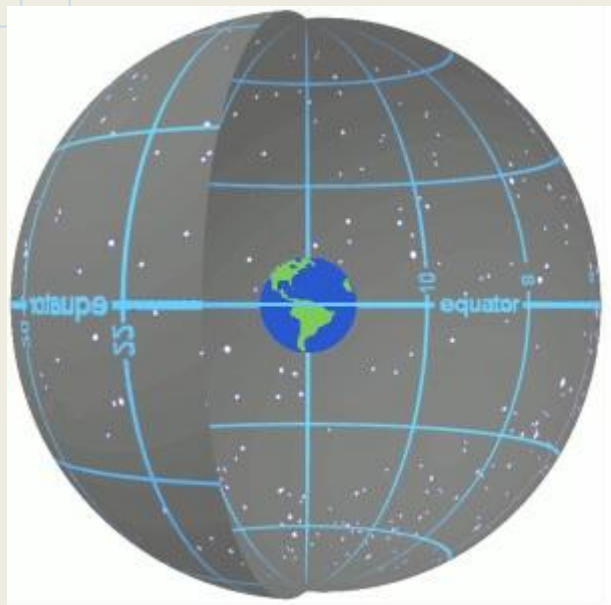
```
if( d < -.9 )
    d = 20. * sqrt(( 1. - .81 ) / ( 1.00001 - d * d ));
else
    d = 2. / ( d + 1.);
```

At first we thought we'd have to convert between coordinates before mapping Chandra target data to our celestial sphere, then we realized the coordinate values we have would work well with D3's mapping capabilities already. R.A./Dec is the "latitude and longitude of the sky," the coordinate systems and range of values are the same.

(<http://www.projectpluto.com/project.htm>)



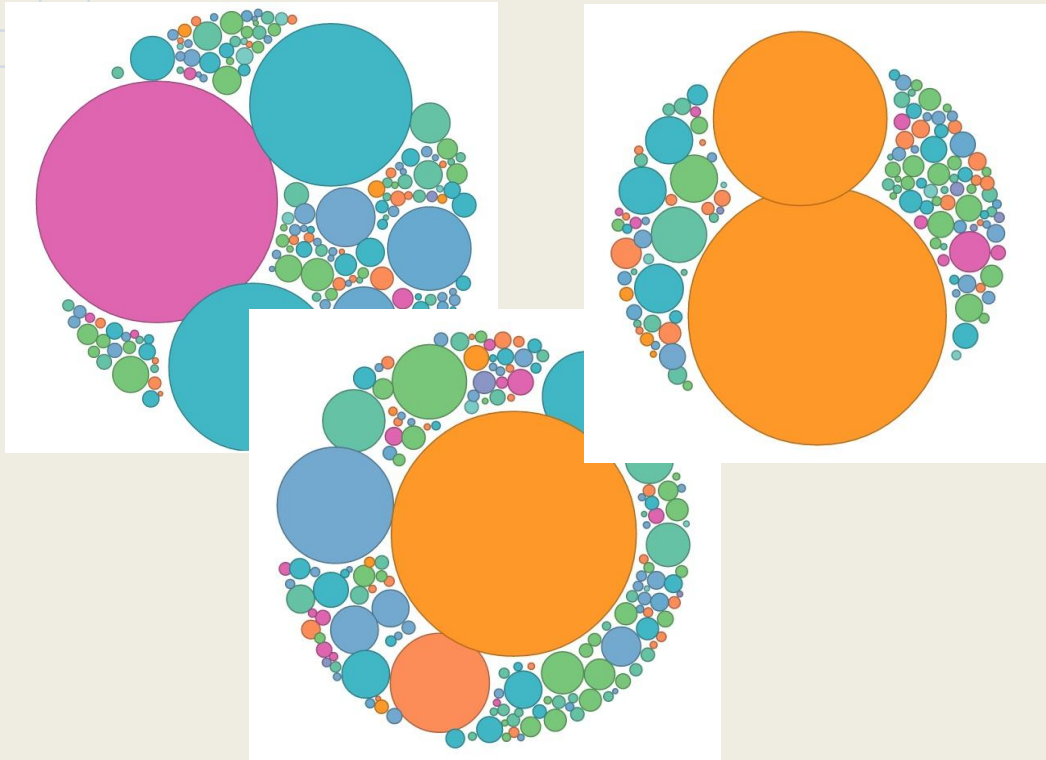
# Calculating the view



So we imagine having two globes, Earth globe nested at the center of our celestial sphere. Earth is populated with lat/long coordinates and celestial sphere is populated with RA/Dec coordinates which we treat like lat/long.



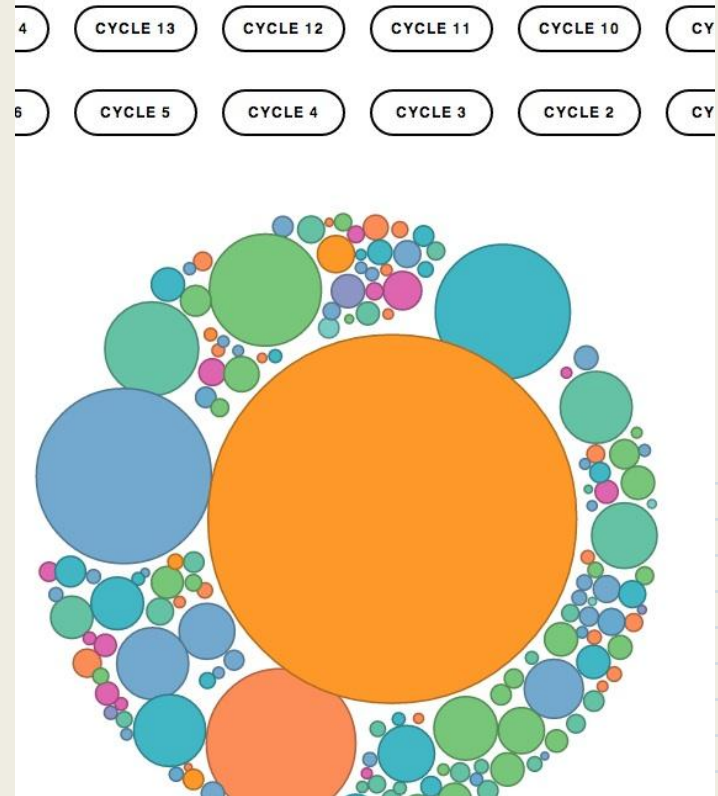
# Penultimate Bubble Design



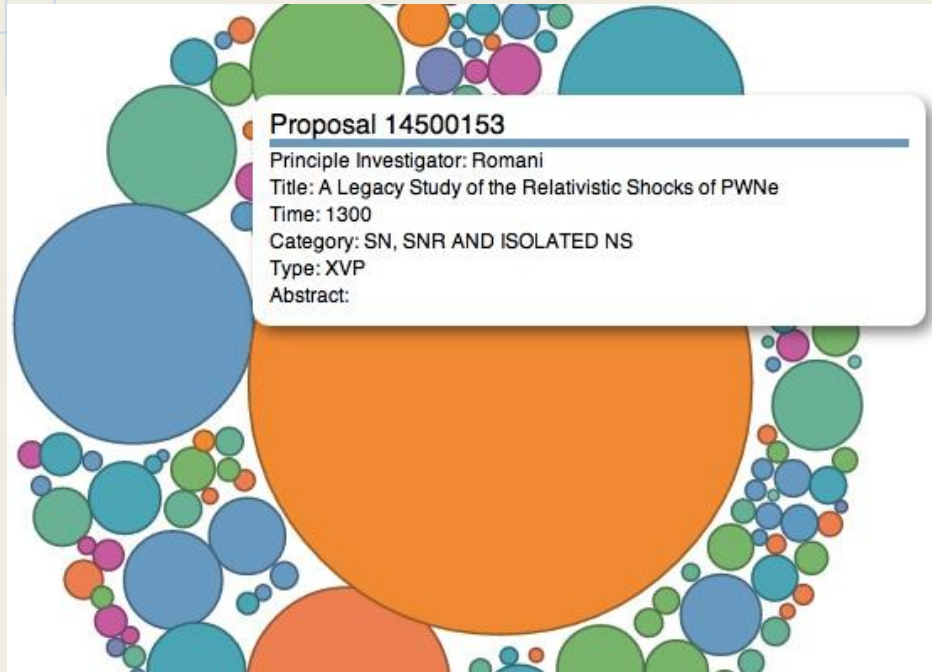
With help from [http://vallandingham.me/bubble\\_charts\\_in\\_d3.html](http://vallandingham.me/bubble_charts_in_d3.html), I decided a force diagram was actually what I wanted, Because the animation was a really nice effect for when you were switching between cycles. Seen to the left are three years of Chandra observations, details on next slide.

# Penultimate Bubble Design

Each bubble represents a science proposal that has been approved for observation on the telescope. Size is the time allotted to each proposal, color corresponds to science category. Above you can see buttons that correspond to each year of observation, to allow the user to explore all cycles.



# Penultimate Bubble Design



More information is revealed on mouse-over events:

- Proposal number
- Lead Scientist
- Proposal Title
- Time (in kiloseconds)
- Science Category
- Type of Observation
- and Abstract (not visible in screen cap)

# Ultimate Bubble Design

The bubbles are integrated into the final project page to the right of the main field of view. If you click on any target or “star” in the sky view, the corresponding bubble chart (yearly observing cycle) that the target was observed in appears on the right. It disappears when an object from another cycle is selected, and is replaced by the new correct cycle. This screen cap was taken in the early stages of integration of the bubbles into the final project page.

current cycle:10

